THE ASTROPHYSICAL JOURNAL, 507:L5–L8, 1998 November 1

FIRST MEASUREMENT OF THE SUBMILLIMETER SUNYAEV-ZELDOVICH EFFECT

J. M. LAMARRE,[1] M. GIARD,[2] E. POINTECOUTEAU,[2] J. P. BERNARD,[1] G. SERRA,[2] F. PAJOT,[1] F. X. DÉSERT,[1] I. RISTORCELLI,[2] J. P. TORRE,[3] S. CHURCH,[4] N. CORON,[1] J. L. PUGET,[1] AND J. J. BOCK[5]

Received 1998 July 27; accepted 1998 August 27; published 1998 September 11

ABSTRACT

We report the first detection of the Sunyaev-Zeldovich (S-Z) increment on the cosmic microwave background at submillimeter wavelengths in the direction of a cluster of galaxies. It was achieved toward the rich cluster Abell 2163, using the PRONAOS 2 m stratospheric telescope. Together with data from the SuZIE, Diabolo, and *ISO*-PHT experiments, these measurements, for the first time, give a complete picture of the far-infrared–to–millimeter spectral energy distribution of the diffuse emission toward a cluster of galaxies. It clearly shows the positive and negative parts of the S-Z effect and also a positive signal at short wavelengths that can be attributed to foreground dust in our Galaxy.

Subject headings: balloons — cosmic microwave background — dust, extinction — galaxies: clusters: individual (A2163) — infrared: general

1. INTRODUCTION

The Sunyaev-Zeldovich (S-Z) effect (Sunyaev & Zeldovich 1972) is a spectral distortion of the cosmic microwave background (CMB) that is due to inverse Compton scattering of CMB photons by hot electrons in clusters of galaxies. It consists of a flux decrement at millimeter and centimeter wavelengths and a flux increment at shorter wavelengths. If the temperature of the electron gas is determined independently, for instance from the X-ray spectrum, then the knowledge of both parts of the S-Z effect can provide information about the intracluster gas mass (thermal effect) and its peculiar velocity with respect to the Hubble flow (kinetic effect). Recent calculations that fully take into account the relativistic effects have shown that for the hottest clusters, $T_e > 8$ keV, the S-Z spectrum departs significantly from the Sunyaev & Zeldovich result (see, e.g., Rephaeli 1995). This temperature dependence of the S-Z spectrum is particularly important in the submillimeter domain. Pointecouteau, Giard, & Barret (1998) have shown that it could be used to determine the electron temperature from future space-borne submillimeter/millimeter S-Z data, without any X-ray data.

From the direct comparison of the cluster's X-ray flux with the amplitude of the S-Z thermal effect, it is possible to derive the cluster's angular distance and thus the Hubble constant. This method is fully independent of the classical distance-scale determination. Several measurements of the decremental part at millimeter or centimeter wavelengths, with derivations of H_0 and peculiar velocities, have been achieved successfully from the ground (see, for instance, Birkinshaw, Hughes, & Arnaud 1991; Jones et al. 1993; Birkinshaw & Hughes 1994; Myers et al. 1997; Holzapfel et al. 1997b, 1997c). The determination of the cluster's peculiar velocity is performed at wavelengths near 1.4 mm, where the thermal effect is close to zero. At this wavelength, the dust emission of a Galactic cirrus or extragalactic starbursts can be significant and pollutes the measurement. Only infrared/submillimeter observations can raise this degeneracy. In this Letter, we report such measurements for the cluster Abell 2163.

This is a well-studied massive cluster located at $z = 0.201$, which has one of the hottest known intracluster gas temperatures ($T_e = 12$–15 keV; Elbaz, Arnaud, & Boehringer 1995 and Markevitch et al. 1996). This makes it a very attractive candidate for measurements of the S-Z effect. High-sensitivity measurements of the S-Z effect on this cluster have been obtained at 1.1, 1.4, and 2.1 mm using the Sunyaev-Zeldovich Infrared Experiment (SuZIE) Caltech photometer on the Caltech Submillimeter Observatory (CSO), Mauna Kea, Hawaii (Holzapfel et al. 1997a).

2. OBSERVATIONS

2.1. *Submillimeter Data*

The submillimeter data presented here were obtained with the PRONAOS telescope[6] (Serra et al. 1998) during a 30 hr stratospheric flight from Fort Sumner, New Mexico, on 1996 September 22 and 23. The 2 m primary dish of the instrument is a six-element segmented mirror with active control of the shape to compensate for in-flight thermal and gravity changes. The SPM photometer (Lamarre et al. 1994) includes warm optics that provide the sky modulation and internal regulated blackbody calibrators. The detector system uses bolometers cooled at 0.3 K with closed cycle ^{3}He coolers inside a liquid ^{4}He cryostat. There are four spectral bands at 170–240, 240–340, 340–540, and 540–1050 μm with beams of $2'$, $2'$, $2'.5$, and $3'.5$ (channels 1–4, respectively). The optical scheme uses dichroics so that a single direction on the sky is observed in the four channels simultaneously.

Our observation strategy includes three levels of beam modulation to subtract the instrumental systematic signals and their possible variations: (i) beam switching at constant elevation, with a $6'$ amplitude, at a frequency of 19.5 Hz, (ii) telescope nodding so that the source is alternately seen in the positive

[1] Institut d'Astrophysique Spatiale, Université Paris XI, Bâtiment 121, 91405 Orsay Cedex, France.

[2] Centre d'Étude Spatiale des Rayonnements, B.P. 4346, F-31028 Toulouse Cedex 4, France.

[3] Service d'Aéronomie du CNRS, BP 3, F-91371 Verrières-le-Buisson Cedex, France.

[4] Department of Physics, Mathematics, and Astronomy, 103-33, California Institute of Technology, CA 91125.

[5] Jet Propulsion Laboratory, California Institute of Technology, MS 169-327, Pasadena, CA 91109.

[6] The PRONAOS telescope is operated under the responsibility of the Centre National d'Études Spatiales (CNES), in collaboration with the laboratories of the authors.

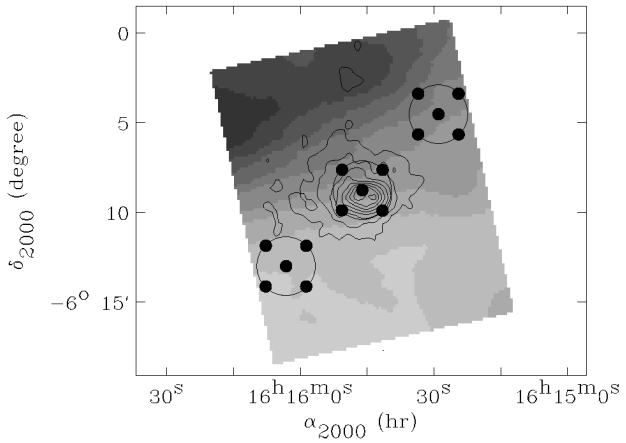

FIG. 1.—Positions observed with PRONAOS overlaid on the 180 μm *ISO*-PHT map (*gray scale*; the minimum and maximum colors are at 15 and 30 MJy sr^{-1}, respectively) and the X-ray *ROSAT* PSPC contours. The dots show the centers of the five observed positions (cluster plus left and right beams at the same elevation), and the circles show the PRONAOS 3.′5 beam FWHM at 630 μm.

and negative beams, at a frequency of about 0.01 Hz, and (iii) repeating the observation on a blank field, with the same duration and observing mode. The blank field was selected in the neighborhood of the cluster, for minimum dust contamination in the *IRAS* 100 μm maps ($\alpha_{50} = 17^{h}17^{m}58^{s}$, $\delta_{50} = 4°36'32''$). Five positions are observed in the direction of the cluster: one at the nominal cluster center (maximum X-ray brightness) and the other four at 1.′6 offsets in elevation and cross-elevation from this center (see Fig. 1). This strategy was chosen to cope with a possible mispointing of the telescope (which did not occur) and to provide information on the cluster extension in case of a high signal-to-noise ratio (S/N) detection. A2163 and the reference field were each observed for a total duration of 54 minutes.

The sensitivities achieved in flight by the PRONAOS-SPM system are 1.0, 0.58, 0.17, and 0.06 MJy sr^{-1}, respectively, in the four channels, for S/N = 1 and an observation time of 1 hr. The noise level in channels 1 and 2 is dominated by low-frequency fluctuations that are likely due to residual atmospheric emissions. These fluctuations are still important in channel 3 but can be removed efficiently by a correlation with channel 1 and the subtraction of the correlated component. The residual noise level is then about 0.09 MJy sr^{-1} in channel 3, which, together with the noise in channel 4, is close to what is expected from photon noise. The calibration is performed in four steps: (i) the ground-based calibration of the photometer on extended blackbodies at different temperatures, (ii) the ground-based measurement of the bands' spectral responses, (iii) the in-flight measurement of the instrument beam on the planet Saturn, and (iv) the in-flight monitoring of the detector response on an internally modulated reference source (a detailed description of the noise analysis and calibration procedures will be published in a forthcoming paper by Pajot et al. 1998). The resulting absolute calibration accuracy has been estimated to be on the order of 10%. Finally, for each analyzed source, the calibration coefficients are recomputed in a self-consistent manner, integrating the bandpass over the best estimate of the source's spectrum (e.g., dust plus the S-Z effect in the case of A2163).

The data processing includes (i) data deglitching and filtering, (ii) demodulation from telescope nodding: (positive$_{\rm beam}$ − negative$_{\rm beam}$)/2, and (iii) averaging. Before averaging, channels 3 and 4 were cross-correlated with channel 1 to subtract any correlated noise component. The correlation ratios found are $F_3/F_1 \simeq 0.06$ and $F_4/F_1 \simeq 0.03$ in units of jansky. These color ratios are much smaller than the cosmic dust emission colors, which will be the main contributor to the flux measured in channel 1: $F_3/F_1 \simeq 0.43$ and $F_4/F_1 \simeq 0.11$ for dust at 15 K with a spectral index of 2. However, since this decorrelation process also implies some subtraction of the dust component from channels 3 and 4, the average data values were self-consistently corrected using the final dust best-fit spectrum ($T \simeq 15$ K).

TABLE 1

NUMERICAL VALUES FOR THE MEASUREMENTS GATHERED IN FIG. 2

λ (μm)	Instrument	Y_c[a] ($\times 10^{-4}$)	Estimated Signal[b] (MJy sr^{-1})
90	*ISO*-PHT	...	0.16 [0.14]
100	*IRAS*	...	0.18 [0.22]
180	*ISO*-PHT	...	1.04 [0.18]
390	PRONAOS	...	0.43 [0.09]
630	PRONAOS	...	0.30 [0.08]
1120	SuZIE	4.05 [1.45][c]	0.107 [0.038]
1380	SuZIE	9.9 [6.0][c]	−0.039 [0.024]
2120	SuZIE	3.73 [0.35][c]	−0.140 [0.013]
2100	Diabolo	5.5 [2.2][d]	−0.20 [0.08]

[a] Central Comptonization parameter taken from the literature (assuming the same King profile as in this Letter).

[b] Estimated signal for a 3.′5 beam and 6′ modulation amplitude (square brackets give 1 σ errors).

[c] Holzapfel et al. 1997b, 1997c.

[d] Désert et al. 1998.

2.2. *Far-Infrared Data*

Maps at 90 and 180 μm were obtained with the PHOT instrument on board the *Infrared Space Observatory* (*ISO*)[7] satellite (open time program: GSERRA:SZCLUST). The observation mode was a PHOT-32 8 × 8 raster map with steps of 92″ and integration times of 20 and 64 s pixel^{-1} (pixel sizes are 43″ and 90″, respectively, for the 90 and 180 μm filters). The data reduction was performed with the PIA-7.01 software.[8] In order to get consistent data that would allow us to derive the dust emission, the PRONAOS observing sequence was simulated with its parameters (beam switching and beam size) on the *ISO* maps (see Fig. 1). The results of these simulated measurements are reported in Table 1 with the corresponding error bars (see also Fig. 2). The error bars have been derived from the rms fluctuation taken on a map of residuals. This map was obtained by the subtraction of the large-scale cirrus pattern that was fitted as a 5° two-dimensional polynomial. The error bar obtained in this manner is always larger than the PHOT absolute calibration uncertainty (10%–20%).

The same operation was performed on the *IRAS* ISSA map at 100 μm. Although the spatial modulation for PRONAOS and SuZIE is not exactly the same, the simulations using the 180 μm *ISO*-PHT data show that the dust signal is the same within error bars. Thus, a single dust signal is used in the interpretation of the data.

[7] An ESA project with instruments funded by ESA Member States (especially the PI countries: France, Germany, the Netherlands, and the UK) with the participation of ISAS and NASA.

[8] PIA is a joint development by the ESA Astrophysics Division and the ISOPHOT Consortium. The ISOPHOT Consortium is led by the Max Planck Institute for Astronomy (MPIA), Heidelberg. Contributing ISOPHOT Consortium institutes are DIAS, RAL, AIP, MPIK, and MPIA.

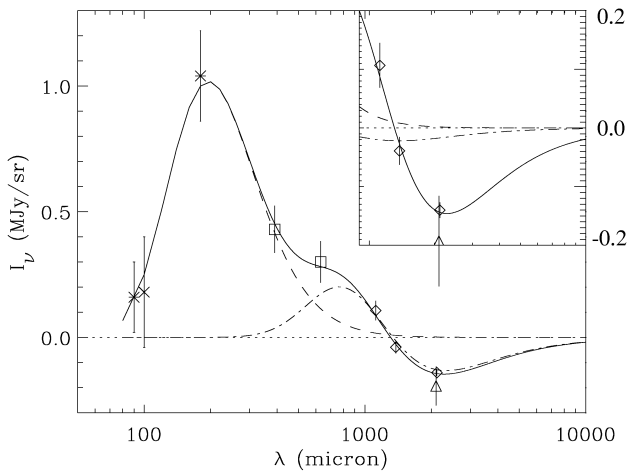

FIG. 2.—Far-infrared–to–millimeter brightness difference between the cluster of galaxies A2163 and its surroundings, using data from *ISO*-PHT (*asterisks*), *IRAS* (*crosses*), PRONAOS (*squares*), SuZIE (*diamonds*), and Diabolo (*triangles*). All values are homogeneous with the PRONAOS dilution (3′.5 beam, 6′ beam throw). The solid line shows the best fit of a model, including the contributions of the foreground dust (*dashed line*), the positive and negative parts of the thermal S-Z effect (*dash-dotted line*), and the kinetic S-Z effect (*dash-dotted line in insert*). The parameters of the fit are the dust temperature $T_d = 14.8 \pm 1$ K, the Comptonization parameter in the direction of the cluster center $Y_C = 3.42^{+0.41}_{-0.46} \times 10^{-4}$, and the cluster peculiar velocity $V_p = 975^{+812}_{-971}$ km s^{-1}, which can also be interpreted as a negative CMB fluctuation of -119^{+99}_{-118} μK.

3. RESULTS AND DISCUSSION

In Figure 2, we show our far-infrared and submillimeter measurements, together with the existing millimeter data from Holzapfel et al. (1997c) at 1.1, 1.4, and 2.1 mm (SuZIE on the CSO telescope: 1′.9 beam, 4′.6 beam throw) and from Désert et al. (1998) at 2.1 mm (Diabolo experiment on the IRAM 30 m telescope: 0′.5 beam, 3′ beam throw). The numerical values with 1 σ error bars are reported in Table 1. The Diabolo and SuZIE data have been corrected for the different beams and modulation amplitudes in order to compare with the PRONAOS data, assuming a King profile for the intracluster gas density:

$$n_{\rm gas}(r) = n_0 \left[1 + \left(\frac{r}{r_c}\right)^2\right]^{-3\beta/2}, \qquad (1)$$

where r_c, the cluster core radius, corresponds to a projected angle $\theta_c = 1'.2$ and $\beta = 0.62$ from Elbaz et al. (1995). The dilution factors for PRONAOS and Diabolo are 0.38 and 0.55, respectively, in terms of the ratio of the beam-averaged signal to the central cluster value. For PRONAOS, this also takes into account averaging over the offset positions. For SuZIE, we use the values derived from single-band fits by Holzapfel et al. (1997c), who use the same cluster model as we do.

Different components appear in this spectrum: the dust shows up at shorter wavelengths and is measured at 90 μm (*ISO*), 100 μm (*IRAS*), 180 μm (*ISO*), and 390 μm (PRONAOS). The S-Z thermal effect has its maximum positive and negative peaks at submillimeter and millimeter wavelengths, respectively. The positive part is measured at 630 μm (PRONAOS) and 1.1 mm (SuZIE), whereas the negative part is measured at 2.1 mm (SuZIE and Diabolo). Finally, the kinetic S-Z effect (or CMB primordial temperature fluctuation; see below) is dominant in the SuZIE 1.4 mm band, where the S-Z thermal effect is close to zero.

We have simultaneously fitted the *ISO*, PRONAOS, Diabolo, and SuZIE data with a S-Z plus dust spectrum having four free parameters: Y_C is the Comptonization parameter in the direction of the cluster center, V_p is the peculiar velocity of the cluster, $F_d(180)$ is the level of dust emission at 180 μm, and T_d is the dust temperature (the dust emissivity index being fixed to $n_d = 2$ from Boulanger et al. 1996). We are not able to distinguish the S-Z kinetic effect from a thermal fluctuation of the CMB itself since they have the same spectrum. In the following, we will quote both the velocity value and the peak ΔT value for a CMB fluctuation that would have the same angular distribution and flux as the cluster S-Z kinetic effect. For the S-Z effect, we assume an intracluster gas temperature of 13 keV and use an exact relativistic thermal S-Z spectrum from Pointecouteau et al. (1998). The best-fit values for the four parameters, using the whole data set and 68% confidence intervals, are $Y_C = 3.42^{+0.41}_{-0.46} \times 10^{-4}$, $V_p = 975^{+812}_{-971}$ km s^{-1} (cluster moving away from us, $\Delta T_{\rm CMB} = -119^{+99}_{-118}$ μK), $F_d(180) = 1.00^{+0.09}_{-0.16}$ MJy sr^{-1}, and $T_d = 14.8 \pm 1$ K. The error bar on each parameter has been calculated from a likelihood analysis after integration over the other parameters: $L = \exp(-\chi^2/2)$. It was not necessary to assume a prior probability for any of the four parameters.

First of all, this data set provides three measurements of the S-Z effect in A2163 that were made with significantly different beam sizes: 3′.5, 1′.9, and 0′.5, respectively, for PRONAOS, SuZIE, and Diabolo. Within the error bars, the three measurements give the same value for the Comptonization parameter in the direction of the cluster center. This validates the King profile that has been derived from the X-ray analysis for the intracluster gas distribution, for a cluster radius ranging from 0.4 to 5 times the core radii.

Our values for the Compton parameter and cluster peculiar velocity can be compared with the values derived in Holzapfel et al. (1997c) from the analysis of the SuZIE data at 1.1, 1.4, and 2.1 mm: $Y_C = 3.73^{+0.47}_{-0.61} \times 10^{-4}$ and $V_p = 490^{+910}_{-730}$ km s^{-1}. However, in their analysis, the authors assumed a zero dust emission level, which is not realistic given the far-infrared measurements. The *ISO* map in Figure 1 clearly shows that this cluster, which is at medium Galactic latitude, lies behind a significant layer of Galactic dust (about 25 MJy sr^{-1} at 180 μm). We show in Figure 3 that the millimeter data do not allow a precise determination of the cluster peculiar velocity in the absence of any submillimeter measurement constraining the dust contribution. This figure displays the 68% and 95% confidence contours on V_p and Y_C, including (*and not including*) the far-infrared and submillimeter data in the fit: solid lines (*dashed lines*). In the second case (*dashed line*), the parameters of the dust component have been varied in the following range: -2 MJy sr^{-1} $< F_d(180\ \mu{\rm m}) < 2$ MJy sr^{-1}, 10 K $< T_d <$ 20 K. This is a plausible range considering the average depth of the cirrus cloud in the direction of A2163: $N_{\rm H} = 1.6 \times 10^{21}$ cm^{-2} from the X-ray data (Elbaz et al. 1995) or $N_{\rm H} = 2.1 \times 10^{21}$ cm^{-2} from 21 cm surveys (Dickey & Lockman 1990). We use the infrared-to-$N_{\rm H}$ colors from Boulanger et al. (1996): 1.26×10^{-20} MJy sr^{-1} cm^2 at 140 μm.

Although it remains within the previous error bars, the velocity change induced by taking into account the dust contribution implies a slight decrease in Y_C. This is true for the following reason: the kinetic S-Z effect contributes about 10% of the measured decrement at 2.1 mm, the wavelength where the thermal S-Z effect is mostly constrained by the data. The

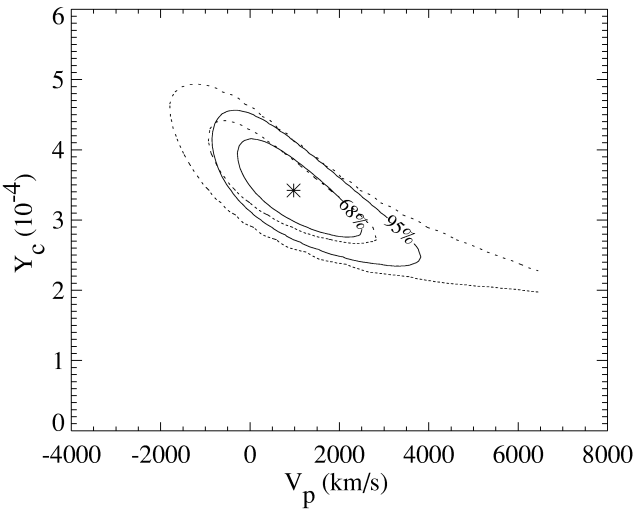

FIG. 3.—The 68% and 95% confidence limits for the determination of the cluster peculiar velocity and central Comptonization parameter from the far-infrared, submillimeter, and millimeter data. The dashed line shows the degraded limits if far-infrared and submillimeter data are ignored, allowing the dust contribution to vary in a plausible range (see text).

combined data set (submillimeter plus millimeter) only slightly improves the precision of the Comptonization parameter since the accuracy of the PRONAOS measurement of the positive S-Z effect (S/N = 3–4) is much less than that of the SuZIE measurement at 2.1 mm (S/N = 10).

Concerning the derivation of H_0 by a comparison of the Comptonization parameter with X-ray fluxes, this scales as F_X/Y^2. Thus, the H_0 ($q_0 = \frac{1}{2}$) value derived by using the same isothermal model for the cluster gas distribution as Holzapfel et al. (1997c) increases from 60^{+40}_{-23} to 71^{+47}_{-27} km s^{-1} Mpc^{-1} with our determination of Y_C.

To conclude, the combined data set presented here (Fig. 2) demonstrates the need for submillimeter data to interpret correctly the S-Z measurements and, more generally, the millimetric CMB data. At this stage, we are not able to assess the origin of the submillimeter dust emission toward A2163: it can be either (i) residual unbalanced Galactic dust as assumed above, (ii) background starburst galaxies that can possibly be magnified by a gravitational lensing effect, or (iii) intracluster dust as measured by Stickel et al. (1998) toward the Coma Cluster. This last hypothesis was examined carefully. Data from *ISO*-PHT show that the measured flux depends on the orientation of the simulated beam switching and that the mean of all possible orientations (1.5 σ detection) does not provide a confirmation of a brightness excess toward the cluster. Moreover, given the depth of the foreground cirrus cloud (see above), the hypothesis of contamination by Galactic dust seems very likely.

The case of A2163, a massive cluster at medium Galactic latitude, actually provides a good illustration of the problems that will be faced when interpreting data for more standard clusters at higher Galactic latitudes [$Y_C \simeq 10^{-5}$, $F_d(180\ \mu\text{m}) \simeq 5$ MJy sr^{-1}] with the future, very sensitive, space-borne instruments such as *Planck* (Bersanelli et al. 1996) and the Far InfraRed and Submillimetre Telescope (FIRST). Submillimeter capabilities, as provided by these two satellites, will be required to derive meaningful peculiar velocities and precisions below 10% on the Comptonization parameter. However, concerning the peculiar velocity, the fundamental limitation will remain the CMB because it has the same spectrum as the S-Z kinetic effect (see, e.g., Haehnelt & Tegmark 1996 and Aghanim et al. 1997). In a similar way, the analysis of the primordial CMB anisotropies themselves, at high angular resolution ($\theta > 5'$) from the *Planck* 217 GHz channel, will also suffer from the dust contamination and will require the help of the submillimeter channels.

We are very indebted to the CNES team led by F. Buisson who were in charge of the development and operations of the PRONAOS gondola and telescope. The professionalism of the NSBF team led by D. Ball was very much appreciated. We are also very grateful to the CNRS technical team led by G. Guyot who were in charge of the focal-plane instrument SPM. We thank W. L. Holzapfel and D. L. Clements for their help and knowledgeable comments.

REFERENCES

Aghanim, N., De Luca, A., Bouchet, F. R., Gispert, R., & Puget, J. L. 1997, A&A, 325, 9
Bersanelli, M., et al. 1996, COBRAS/SAMBA, ESA Rep. on Phase A Study, D/SCI(96)3 (Noordwijk: ESA)
Birkinshaw, M., & Hughes, J. P. 1994, ApJ, 420, 33
Birkinshaw, M., Hughes, J. P., & Arnaud, K. A. 1991, ApJ, 379, 466
Boulanger, F., et al. 1996, A&A, 312, 256
Désert, F. X., et al. 1998, NewA, in press
Dickey, J. M., & Lockman, F. J. 1990, ARA&A, 28, 215
Elbaz, D., Arnaud, M., & Boehringer, H. 1995, A&A, 293, 337
Haehnelt, M. G., & Tegmark, M. 1996, MNRAS, 279, 545
Holzapfel, W. L., et al. 1997a, ApJ, 479, 17
———. 1997b, ApJ, 480, 449
———. 1997c, ApJ, 481, 35
Jones, M., et al. 1993, Nature, 365, 320
Lamarre, J. M., et al. 1994, Infrared Phys., 35, 277
Markevitch, M., Mushotzky, R., Inoue, H., Yamashita, K., Furuzawa, A., & Tawara, Y. 1996, ApJ, 456, 437
Myers, S. T., Baker, J. E., Readhead, A. C. S., Leitch, E. M., & Herbig, T. 1997, ApJ, 485, 1
Pajot, F., et al. 1998, in preparation
Pointecouteau, E., Giard, M., & Barret, D. 1998, A&A, in press
Rephaeli, Y. 1995, ApJ, 445, 33
Serra, G., et al. 1998, in Proc. ICSO Conf., Toulouse, Poster Session 2
Stickel, M., Lemke, D., Mattila, K., Haikala, L. K., & Haas, M. 1998, A&A, 329, 55
Sunyaev, R., & Zeldovich, Ya. B. 1972, Comments Astrophys. Space Phys., 4, 173